

Emergent symmetries in atomic nuclei: Probing nuclear dynamics and physics beyond the standard model

K. D. Launey^{1*}, K. S. Becker¹, G. H. Sargsyan^{1,2}, O. M. Molchanov¹, M. Burrows¹, A. Mercenne¹, T. Dytrych^{1,3}, D. Langr⁴ and J. P. Draayer¹

¹ Department of Physics and Astronomy, Louisiana State University, Baton Rouge, LA 70803, USA

² Lawrence Livermore National Laboratory, Livermore, California 94550, USA

³ Nuclear Physics Institute of the Czech Academy of Sciences, 250 68 Řež, Czech Republic

⁴ Department of Computer Systems, Faculty of Information Technology, Czech Technical University in Prague, 16000 Praha, Czech Republic

* klauney@lsu.edu

December 16, 2022

1

2



34th International Colloquium on Group Theoretical Methods in Physics
Strasbourg, 18-22 July 2022
doi:[10.21468/SciPostPhysProc.7](https://doi.org/10.21468/SciPostPhysProc.7)

3 Abstract

4 Dominant shapes naturally emerge in atomic nuclei from first principles, thereby es-
5 tablishing the shape-preserving symplectic $Sp(3, \mathbb{R})$ symmetry as remarkably ubiquitous
6 and almost perfect symmetry in nuclei. We discuss the critical role of this emergent
7 symmetry in enabling machine-learning descriptions of heavy nuclei, *ab initio* modeling
8 of α clustering and collectivity, as well as tests of beyond-the-standard-model physics.
9 In addition, the $Sp(3, \mathbb{R})$ and $SU(3)$ symmetries provide relevant degrees of freedom
10 that underpin the *ab initio* symmetry-adapted no-core shell model with the remarkable
11 capability of reaching nuclei and reaction fragments beyond the lightest and close-to-
12 spherical species.

13

14 Contents

15	1 Introduction	2
16	2 Emergent symmetries in nuclei: $Sp(3, \mathbb{R})$ and $SU(3)$	3
17	2.1 $SU(3)$ scheme	3
18	2.2 $Sp(3, \mathbb{R})$ scheme	4
19	2.3 <i>Ab initio</i> symmetry-adapted no-core shell model	7
20	3 Critical Role of Symmetries for Studies and Predictions of Nuclear Properties	8
21	3.1 Machine learning pattern recognition with the SA-NGSM	8
22	3.2 Probing clustering and physics beyond the standard model	9
23	3.3 Optical potential in the symmetry-adapted framework for nuclear reactions	10
24	4 Conclusion	11

26

27

28 **1 Introduction**

29 Dominant shapes, often very few in number, naturally emerge in atomic nuclei. This remark-
 30 able result has been recently shown by large-scale nuclear simulations from first principles [1].
 31 Indeed, each nuclear shape respects an exact symmetry, namely, the symplectic $\text{Sp}(3, \mathbb{R})$ sym-
 32 metry [2, 3]. Thereby the outcome of these simulations establishes the symplectic $\text{Sp}(3, \mathbb{R})$
 33 symmetry as remarkably ubiquitous and almost perfect symmetry in nuclei up through the
 34 calcium region (anticipated to hold even stronger in heavy nuclei [4]). This outcome also
 35 exposes for the first time the fundamental role of the $\text{Sp}(3, \mathbb{R})$ symmetry and suggests that its
 36 origin is rooted in the strong nuclear force, in the low-energy regime.

37 This builds upon a decades-long research, starting with the pivotal work of Draayer [5, 3,
 38 6, 7] and that of Rowe and Rosensteel [2, 8, 4, 9], who have successfully harnessed group the-
 39 ory as a powerful tool for understanding and computing the intricate structure of nuclei. This
 40 pioneering work has been instrumental in designing the theory that underpins many highly
 41 ordered patterns unveiled amidst the large body of experimental data [10, 11, 12]. In addi-
 42 tion, it has explained phenomena observed in energy spectra, $E2$ transitions and deformation,
 43 giant resonances (GR), scissor modes and $M1$ transitions, electron scattering form factors, as
 44 well as the interplay of pairing with collectivity. The new developments and insights have
 45 provided the critical structure raised upon the very foundation laid by Elliott [13, 14, 15]
 46 and Hecht [16, 17], and opened the path for large-scale calculations feasible today on super-
 47 computers. And while these earlier algebraic models have been very successful in explaining
 48 dominant nuclear patterns, they have assumed symmetry-based approximations and have of-
 49 ten neglected symmetry mixing. This establishes $\text{Sp}(3, \mathbb{R})$ as an *effective symmetry*¹ for nuclei,
 50 which may or may not be badly broken in realistic calculations. It is then imperative to probe
 51 if this symmetry naturally arises within an *ab initio* framework, which will, in turn, establish
 52 its fundamental role.

53 Indeed, within an *ab initio* framework without *a priori* symmetry assumptions, the symmetry-
 54 adapted no-core shell model (SA-NCSM) [19, 20, 7] with chiral effective field theory (EFT)
 55 interactions [21, 22, 23] has recently confirmed the goodness of the symplectic $\text{Sp}(3, \mathbb{R})$ sym-
 56 metry that is only slightly broken. With no parameters to adjust, the SA-NCSM is capable
 57 then not only to explain but also to predict the emergence of nuclear shapes and collectivity
 58 across nuclei, even in close-to-spherical nuclear states without any recognizable rotational
 59 properties.

60 Within an *ab initio* framework, the emergent symmetries play a critical role, as they can
 61 inform relevant degrees of freedom. In particular, a symmetry-adapted many-body basis can
 62 be employed, as in the SA-NCSM, thereby providing solutions for drastically reduced sizes of
 63 the spaces in which particles reside (referred to as “model spaces”) compared to the corre-
 64 sponding ultra-large model spaces, without compromising the accuracy of results for various
 65 nuclear observables. By exploiting symplectic symmetry, *ab initio* descriptions of spherical
 66 and deformed nuclei up through the calcium region are now possible without the use of effec-
 67 tive charges [20, 24, 25, 7, 26]. This allows the SA-NCSM to accommodate even larger model

¹ A familiar example for an effective symmetry is $\text{SU}(3)$. While the Elliott model with a single $\text{SU}(3)$ irrep explains ground-state rotational states in deformed nuclei, the $\text{SU}(3)$ symmetry is, in general, largely mixed, mainly due to the spin-orbit interaction (nonetheless, $\text{SU}(3)$ has been shown to be an excellent quasi-dynamical symmetry, that is, each rotational state has almost the same $\text{SU}(3)$ content [18]).

68 spaces and to reach heavier nuclei, such as ^{20}Ne [1], ^{21}Mg [27], ^{22}Mg [28], ^{28}Mg [29], as
 69 well as ^{32}Ne and ^{48}Ti [30].

70 In this paper, we briefly outline the $\text{SU}(3)$ and $\text{Sp}(3, \mathbb{R})$ schemes utilized by the *ab ini-*
 71 *tio* SA-NCSM. We overview the critical role of the emergent $\text{Sp}(3, \mathbb{R})$ symmetry in enabling
 72 machine-learning descriptions of heavy nuclei [31], *ab initio* modeling of α clustering and col-
 73 lectivity, along with tests of beyond-the-standard-model physics [32]. In addition, we show
 74 that with the help of the SA-NCSM, which expands *ab initio* applications up to medium-mass
 75 nuclei by using the dominant symmetry of nuclear dynamics, one can provide solutions to
 76 reaction processes in this region, with a focus on elastic neutron scattering.

77 2 Emergent symmetries in nuclei: $\text{Sp}(3, \mathbb{R})$ and $\text{SU}(3)$

78 2.1 $\text{SU}(3)$ scheme

79 It is well known that $\text{SU}(3)$ [13, 33, 5, 34, 17] is the symmetry group of the spherical har-
 80 monic oscillator (HO) that underpins the valence-shell model and the valence-shell $\text{SU}(3)$
 81 (Elliott) model [13, 14, 15] (for technical details of $\text{SU}(3)$, see Ref. [35]). The Elliott model
 82 has been shown to naturally describe rotations of a deformed nucleus without the need for
 83 breaking rotational symmetry. But even beyond the valence shell, the $\text{SU}(3)$ scheme pro-
 84 vides a classification of the complete shell-model space in multiple shells, and is related to
 85 the *LS*-coupling and *jj*-coupling schemes via a unitary transformation. It divides the space
 86 into basis states of definite $(\lambda \mu)$ quantum numbers of $\text{SU}(3)$ that are linked to the intrinsic
 87 quadrupole deformation according to the established mapping [36, 37, 38]. For example, the
 88 simplest cases, (00) , $(\lambda 0)$, and (0μ) , describe spherical, prolate, and oblate deformation,
 89 respectively², while a general nuclear state is typically a superposition of several hundred
 90 various triaxially deformed configurations. Note that, in this respect, basis states can have
 91 little to no deformation, and, e.g., about 60% of the ground state of the closed-shell ^{16}O is
 92 described by a single $\text{SU}(3)$ basis state, the spherical (00) .

93 Specifically, in the $\text{SU}(3)$ scheme, in place of the spherical quantum numbers $|\eta l m_l\rangle$, one
 94 can consider the single-particle HO basis $|\eta_z \eta_x \eta_y\rangle$, the HO quanta in the three Cartesian
 95 directions, z , x , and y , with $\eta_x + \eta_y + \eta_z = \eta$ ($\eta = 0, 1, 2, \dots$ for s, p, sd, \dots shells).
 96 For a given HO major shell, the complete shell-model space is then specified by all distin-
 97 guishable distributions of η_z, η_x and η_y . E.g., for $\eta = 2$, there are 6 different distributions,
 98 $(\eta_z, \eta_x, \eta_y) = (2, 0, 0), (1, 1, 0), (1, 0, 1), (0, 2, 0), (0, 1, 1)$ and $(0, 0, 2)$. The number of these
 99 configurations is $\Omega_\eta = (\eta + 1)(\eta + 2)/2$ (spatial degeneracy) and the associated symmetry is
 100 described by the $U(\Omega_\eta)$ unitary group. Each of these (η_z, η_x, η_y) configurations can be either
 101 unoccupied or has maximum of two particles with spins $\uparrow\downarrow$.

102 As a simple example for an $\text{SU}(3)$ -scheme basis state, consider $A = 2$ protons in the sd
 103 shell ($\eta = 2$) with a particle in the $(2, 0, 0)$ level with spin \uparrow and another in the $(1, 1, 0)$ level
 104 with spins \uparrow . The total number of quanta in each direction is $(\eta_z^{\text{tot}}, \eta_x^{\text{tot}}, \eta_y^{\text{tot}}) = (3, 1, 0)$, or
 105 equivalently, $\eta^{\text{tot}}(\lambda \mu) = 4(21)$, where $\eta^{\text{tot}} = \eta_x^{\text{tot}} + \eta_y^{\text{tot}} + \eta_z^{\text{tot}}$, together with $\lambda = \eta_z^{\text{tot}} - \eta_x^{\text{tot}}$ and
 106 $\mu = \eta_x^{\text{tot}} - \eta_y^{\text{tot}}$ labeling an $\text{SU}(3)$ irrep, in addition to the total intrinsic spin and its projection
 107 SM_S . For given $(\lambda \mu)$, the quantum numbers κ , L and M_L are given by Elliott [13, 14], accord-
 108 ing to the $\text{SU}(3) \supset \text{SO}(3)_L \supset \text{SO}(2)_{M_L}$, where the label κ distinguishes multiple occurrences
 109 of the same orbital momentum L in the parent irrep $(\lambda \mu)$. For our example, $(\lambda \mu) = (21)$
 110 with $\kappa = 1$, $L = 1, 2, 3$, and $M_L = -L, -L + 1, \dots, L$. Hence, the set $\{\eta^A(\lambda \mu)\kappa(LS)JM\}$

² Following this mapping, quadrupole moments of (00) , $(\lambda 0)$, and (0μ) configurations – in a simple classical
 analogy to rotating spherical, prolate, and oblate spheroids in the lab frame [39] – are zero, negative, and positive,
 respectively.

111 completely labels a 2-proton SU(3)-scheme basis state (with $\eta^{\text{tot}} = A\eta$). A basis state in
 112 this scheme for a 2-particle system is given by, $\{a_{(\eta 0)st_z}^\dagger \times a_{(\eta' 0)s't'_z}^\dagger\}^{(\lambda \mu)\kappa(LS)JM} |0\rangle$, which
 113 is an SU(3)-coupled product, provided that a^\dagger is a proper SU(3) tensor; incidentally, the
 114 SU(3) tensor a^\dagger of rank $(\lambda \mu) = (\eta 0)$ coincides with the familiar particle creation operator,
 115 $a_{(\eta 0)lms\sigma t_z}^\dagger \equiv a_{\eta lms\sigma t_z}^\dagger$, while the particle annihilation SU(3) tensor of rank $(\lambda \mu) = (0 \eta)$ is
 116 given as $\tilde{a}_{(0 \eta)l-ms-\sigma t_z} = (-1)^{\eta+l-m+s-\sigma} a_{\eta lms\sigma t_z}$. Note that for $\eta = \eta' = 2$, e.g., there are only
 117 a few 2-proton configurations $(\lambda \mu) = (4 0)$ with $L = 0, 2, 4$, $(2 1)$ with $L = 1, 2, 3$, and $(0 2)$
 118 with $L = 0, 2$. Furthermore, these basis states are related to LS -coupled basis states (similarly,
 119 to jj -coupled basis states) via a simple unitary transformation,

$$\{a_{(\eta 0)st_z}^\dagger \times a_{(\eta' 0)s't'_z}^\dagger\}^{(\lambda \mu)\kappa(LS)JM} |0\rangle = \sum_{l,l'} \langle (\eta 0)l; (\eta' 0)l' | (\lambda \mu)\kappa L \rangle \{a_{\eta lst_z}^\dagger \times a_{\eta' l's't'_z}^\dagger\}^{(LS)JM} |0\rangle, \quad (1)$$

120 where $\langle \dots; \dots | \dots \rangle$ is the SU(3) analog of the familiar reduced Clebsch-Gordan coefficient
 121 [note that there is no dependence on the particle orbital momenta, l and l' , in the SU(3)-
 122 scheme basis states].

123 An important feature of the SU(3) scheme is that all possible configurations within a
 124 major HO shell η (for protons or neutrons) are not constructed using the tedious procedure of
 125 coupling of creation operators referenced above, but are readily available based on the $U(\Omega_\eta)$
 126 unitary group of the many-body three-dimensional HO. In particular, the basis construction is
 127 implemented according to the reduction [40]

$$\begin{array}{c} U(\Omega_\eta) \\ [f_1, f_2, \dots, f_{\Omega_\eta}] \\ \cup \\ SU(3) \\ (\lambda_\eta \mu_\eta) \end{array} \times \begin{array}{c} SU(2) \\ S_\eta \\ \alpha_\eta \end{array}, \quad (2)$$

128 with $SU(3)_{(\lambda_\eta \mu_\eta)} \supset_{\kappa_\eta} SO(3)_{L_\eta} \supset SO(2)_{M_{L_\eta}}$ [13, 14], where a multiplicity index α_η distinguishes
 129 multiple occurrences of an SU(3) irrep $(\lambda_\eta \mu_\eta)$ in a given $U(\Omega_\eta)$ irrep labeled by Young
 130 tableaux, $[f] = [f_1, f_2, \dots, f_{\Omega_\eta}]$, with $f_1 \geq f_2 \geq \dots \geq f_{\Omega_\eta}$ and $f_i = 0$ (unoccupied), 1 (oc-
 131 cupied by a particle), or 2 (occupied by 2 particles of spins $\uparrow\downarrow$). An illustrative example for 4
 132 particles in the pf shell ($\eta = 3$) is shown in Table 1.

133 2.2 Sp(3, \mathbb{R}) scheme

134 The key role of deformation in nuclei and the coexistence of low-lying quantum states in
 135 a single nucleus characterized by configurations with different quadrupole moments [10]
 136 makes the quadrupole moment a dominant fundamental property of the nucleus. Hence,
 137 the quadrupole moment Q (or deformation) and the monopole moment r^2 (or “size” of the
 138 nucleus), along with nuclear masses, establishes the energy scale of the nuclear problem.
 139 Indeed, the nuclear monopole and quadrupole moments underpin the essence of symplectic
 140 Sp(3, \mathbb{R}) symmetry.

141 Specifically, for A particles in three-dimensional space, the complete basis for the shell
 142 model is described by Sp(3A, \mathbb{R}) \times U(4) [9], where Sp(3A, \mathbb{R}) is the group of all linear canon-
 143 ical transformations of the 3A-particle phase space and Wigner’s supermultiplet group U(4)
 144 describes the complementary spin-isospin space. A complete translationally invariant shell-

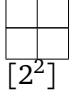
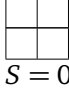
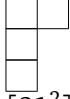
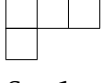


Spatial d.o.f.		Spin d.o.f.
U(10) [$f_1 f_2 \dots f_{10}$]	\supset SU(3) ($\lambda \mu$)	SU(2) S
	(8 2), (7 1), (4 4) ² , (5 2), (0 6), (6 0), (3 3) (1 4), (4 1), (2 2) ² , (1 1)	 $S = 0$
	(9 0), (6 3), (7 1), (4 4), (2 5), (5 2) ² , (3 3) ² (1 4) ² , (4 1) ² , (2 2), (0 3), (3 0) ² , (1 1)	 $S = 1$
	(5 2), (0 6), (3 3), (2 2), (3 0)	 $S = 2$

Table 1: $SU(3) \times SU(2)_S$ configurations for 4 protons (neutrons) in the pf shell ($\eta = 3$ with $\Omega_\eta = 10$). Note that a spatial symmetry represented by a Young tableau $[f_1, \dots, f_{\Omega_\eta}]$ is uniquely determined by its complementary spin symmetry of a given intrinsic spin S_η (conjugate Young tableaux) ensuring the overall antisymmetrization of each $U(\Omega_\eta) \times SU(2)_{S_\eta}$ configuration with respect to spatial and spin degrees of freedom (d.o.f.) [40].

145 model basis is classified according to (see, e.g., [4, 9]),

$$\begin{array}{ccc} \text{Sp}(3(A-1), \mathbb{R}) & \times & \text{U}(4) \\ \cup & & \cup \\ \text{Sp}(3, \mathbb{R}) \times \text{O}(A-1) & & \text{SU}(2)_S \times \text{SU}(2)_T \end{array} \quad (3)$$

146 The $\text{Sp}(3, \mathbb{R})$ scheme utilizes the symplectic group $\text{Sp}(3, \mathbb{R})$. It consists of all *particle-independent*
147 linear canonical transformations of the single-particle phase-space observables, the positions
148 \vec{r}_i and momenta \vec{p}_i (with particle index $i = 1, \dots, A$ and spacial directions $\alpha, \beta = x, y, z$)

$$r'_{i\alpha} = \sum_{\beta} A_{\alpha\beta} r_{i\beta} + B_{\alpha\beta} p_{i\beta} \quad (4)$$

$$p'_{i\alpha} = \sum_{\beta} C_{\alpha\beta} r_{i\beta} + D_{\alpha\beta} p_{i\beta} \quad (5)$$

149 that preserve the Heisenberg commutation relations $[r_{i\alpha}, p_{j\beta}] = i\hbar \delta_{ij} \delta_{\alpha\beta}$ [4, 41, 7]. Gen-
150 erators of these transformations, symbolically denoted as matrices **A**, **B**, **C**, and **D**, are con-
151 structed as “quadratic coordinates” in phase space, \vec{r}_i and \vec{p}_i , and, most importantly, sum
152 over all the particles and act on the space orientation. Hence, the generators include phys-
153 ically relevant operators: the total kinetic energy ($\frac{p^2}{2} = \frac{1}{2} \sum_i \vec{p}_i \cdot \vec{p}_i$), the monopole moment
154 ($r^2 = \sum_i \vec{r}_i \cdot \vec{r}_i$), the quadrupole moment ($Q_{2M} = \sqrt{16\pi/5} \sum_i r_i^2 Y_{2M}(\hat{r}_i)$), the orbital momen-
155 tum ($\vec{L} = \sum_i \vec{r}_i \times \vec{p}_i$), and the many-body harmonic oscillator Hamiltonian ($H_0 = \frac{p^2}{2} + \frac{r^2}{2}$).
156 In addition, other generators describe multi-shell collective vibrations and vorticity degrees of
157 freedom for a description from irrotational to rigid rotor flows.

158 On the contrary, the generators of the complementary $O(A)$ sum over the three spatial
 159 directions and act on the particle index, with a growing complexity with increasing parti-
 160 cle number. One can then organize the A -particle model space according to the dual group
 161 $O(A-1)$, with $O(A) \supset O(A-1) \supset S_A$. The $O(A)$ is the group of orthogonal transformations that
 162 act on the "particle-index" space (transformations of nucleon coordinates, $r_{i\alpha} \rightarrow \sum_{j=1}^A r_{j\alpha} P_{ji}$,
 163 that leave the $O(A)$ scalars $r_\alpha \cdot r_\beta = \sum_{i=1}^A r_{i\alpha} r_{i\beta}$ invariant for $\alpha, \beta = x, y, z$). This scheme is
 164 reviewed in detail in Refs. [4, 9]. $O(A-1)$ is the subgroup of $O(A)$ which leaves center-of-
 165 mass coordinates invariant (note that center-of-mass coordinates are symmetric with respect
 166 to nucleon indices and, therefore, invariant under S_A permutations) and has as a subgroup
 167 the permutation group S_A , which permutes the spatial coordinates of a system of A particles.

168 The $\text{Sp}(3, \mathbb{R})$ scheme utilizes an important group reduction to classify many-particle basis
 169 states $|\sigma n \rho \omega \kappa L M\rangle$ of a symplectic irrep,

$$\text{Sp}(3, \mathbb{R}) \supset U(3) \supset \text{SO}(3) \supset \text{SO}(2) \quad (6)$$

$$\sigma \quad n\rho \quad \omega \quad \kappa \quad L \quad M$$

170 where $\sigma \equiv N_\sigma (\lambda_\sigma \mu_\sigma)$ labels the $\text{Sp}(3, \mathbb{R})$ irrep, $n \equiv N_n (\lambda_n \mu_n)$, $\omega \equiv N (\lambda_\omega \mu_\omega)$, and
 171 $N = N_\sigma + N_n$ is the total number of HO quanta (ρ and κ are multiplicity labels) [4]. The rela-
 172 tion of these symplectic basis states to M -scheme states of the NCSM is provided in Ref. [42].
 173 Importantly, a single-particle $\text{Sp}(3, \mathbb{R})$ irrep spans *all* positive-parity (or negative-parity) states
 174 for a particle in a three-dimensional spherical or triaxial (deformed) harmonic oscillator.

175 The translationally invariant (intrinsic) symplectic $\text{Sp}(3, \mathbb{R})$ generators can be written as
 176 $\text{SU}(3)$ tensor operators in terms of the harmonic oscillator raising, $b_{i\alpha}^{\dagger(10)} = \frac{1}{\sqrt{2}}(r_{i\alpha} - ip_{i\alpha})$,
 177 and lowering $b^{(01)}$ dimensionless operators (with \mathbf{r} and \mathbf{p} the laboratory-frame position and
 178 momentum coordinates and $\alpha = 1, 2, 3$ for the three spatial directions),

$$A_{\mathcal{L}M}^{(20)} = \frac{1}{\sqrt{2}} \sum_{i=1}^A \{b_i^\dagger \times b_i\}_{\mathcal{L}M}^{(20)} - \frac{1}{\sqrt{2}A} \sum_{s,t=1}^A \{b_s^\dagger \times b_t\}_{\mathcal{L}M}^{(20)} \quad (7)$$

$$C_{\mathcal{L}M}^{(11)} = \sqrt{2} \sum_{i=1}^A \{b_i^\dagger \times b_i\}_{\mathcal{L}M}^{(11)} - \frac{\sqrt{2}}{A} \sum_{s,t=1}^A \{b_s^\dagger \times b_t\}_{\mathcal{L}M}^{(11)},$$

$$H_{00}^{(00)} = \sqrt{3} \sum_i \{b_i^\dagger \times b_i\}_{00}^{(00)} - \frac{\sqrt{3}}{A} \sum_{s,t} \{b_s^\dagger \times b_t\}_{00}^{(00)} + \frac{3}{2}(A-1), \quad (8)$$

179 together with $B_{\mathcal{L}M}^{(02)} = (-)^{\mathcal{L}-M} (A_{\mathcal{L}-M}^{(20)})^\dagger$ ($\mathcal{L} = 0, 2$), where the sums run over all A particles of
 180 the system. Equivalently, the symplectic generators, being one-body-plus-two-body operators
 181 can be expressed in terms of the fermion creation operator $a_{(\eta 0)}^\dagger$ and its $\text{SU}(3)$ -conjugate
 182 annihilation operator, $\tilde{a}_{(0 \eta)}$. This is achieved by using the known matrix elements of the
 183 position and momentum operators in a HO basis, and hence, e.g., the first sum of $A_{\mathcal{L}M}^{(20)}$ in Eq.

184 (7) becomes, $\sum_\eta \sqrt{\frac{(\eta+1)(\eta+2)(\eta+3)(\eta+4)}{12}} \{a_{(\eta+2 0)}^\dagger \times \tilde{a}_{(0 \eta)}\}_{\mathcal{L}M}^{(20)}$ [43]. Note that this operator
 185 describes excitations of a nucleon from the η shell to the $\eta + 2$ shell, which corresponds
 186 to creating two single-particle HO excitation quanta, as manifested in the first term of Eq.
 187 (7). The eight $0\hbar\Omega$ operators $C_{\mathcal{L}M}^{(11)}$ ($\mathcal{L} = 1, 2$) generate the $\text{SU}(3)$ subgroup of $\text{Sp}(3, \mathbb{R})$.
 188 They realize the angular momentum operator (dimensionless), $L_{1M} = C_{1M}^{(11)}$, and the Elliott
 189 "algebraic" quadrupole moment tensor $\mathcal{Q}_{2M}^a = \sqrt{3} C_{2M}^{(11)}$.

190 The many-body basis states of an $\text{Sp}(3, \mathbb{R})$ irrep are built over a bandhead $|\sigma\rangle$ (defined by
 191 the usual requirement that the symplectic lowering operators $B_{\mathcal{L}M}^{(02)}$ annihilate it) by $2\hbar\Omega$ 1p-
 192 1h monopole or quadrupole excitations, realized by the first term in $A_{\mathcal{L}M}^{(20)}$ of Eq. (7), together

193 with a smaller $2\hbar\Omega$ 2p-2h correction for eliminating the spurious center-of-mass (CM) motion,
 194 realized by the second term in $A_{\mathcal{L}M}^{(20)}$:

$$|\sigma n \rho \omega \kappa (LS_{\sigma}) JM\rangle = \sum_{M_L M_S} \langle LM_L; S_{\sigma} M_S | JM \rangle \{A^{(20)} \times A^{(20)} \dots \times A^{(20)}\}^n \times |\sigma; S_{\sigma} M_S\rangle_{\kappa LM_L}^{\rho \omega}. \quad (9)$$

195 States within a symplectic irrep have the same spin value, which are given by the spin S_{σ}
 196 of the bandhead $|\sigma; S_{\sigma}\rangle$. Symplectic basis states span the entire shell-mode space. A com-
 197 plete set of labels includes additional quantum numbers $|\{\alpha\}\sigma\rangle$ that distinguish different
 198 bandheads with the same $N_{\sigma}(\lambda_{\sigma} \mu_{\sigma})$. Remarkably, these $\text{Sp}(3, \mathbb{R})$ basis states are in one-
 199 to-one correspondence with a coupled product of the states of the Bohr vibrational model
 200 (realized in terms of giant monopole-quadrupole resonance states with irrotational flows),
 201 $\{A^{(20)} \times A^{(20)} \dots \times A^{(20)}\}^n \times |N_{\sigma}(00)\rangle^{(\lambda_n \mu_n)}$, and $(\lambda_{\sigma} \mu_{\sigma})$ deformed states of an $\text{SU}(3)$
 202 model [41].

203 2.3 *Ab initio* symmetry-adapted no-core shell model

204 Not surprisingly, the symplectic $\text{Sp}(3, \mathbb{R})$ symmetry, the underlying symmetry of the symplectic
 205 rotor model [2, 4], has been found to play a key role across the nuclear chart – from the lightest
 206 systems [44, 45], through intermediate-mass nuclei [3, 46, 7], up to strongly deformed nuclei
 207 of the rare-earth and actinide regions [4, 47, 48, 18]. The results agree with experimental
 208 evidence that supports formation of enhanced deformation and clusters in nuclei, as well as
 209 vibrational and rotational patterns, as suggested by energy spectra, electric monopole and
 quadrupole transitions, radii and quadrupole moments [10, 28, 49].

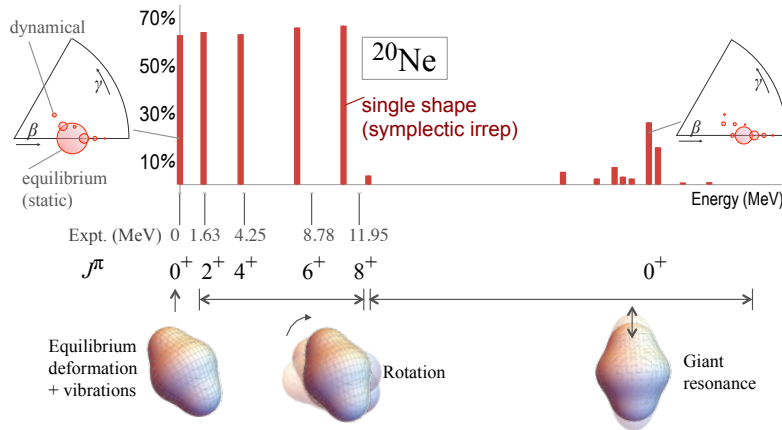


Figure 1: Emergence of almost perfect symplectic $\text{Sp}(3, \mathbb{R})$ symmetry in nuclei from first principles, enabling *ab initio* descriptions of collectivity and clustering. Figure adapted from [1].

210

211 The symmetry-adapted no-core shell model [19, 7, 1] capitalizes on these findings and
 212 presents solutions in terms of a physically relevant basis of nuclear shapes. It exploits both
 213 the $\text{SU}(3)$ and $\text{Sp}(3, \mathbb{R})$ schemes. Indeed, since the symplectic symmetry does not mix nuclear
 214 shapes, the novel nuclear feature provides important insight from first principles into the
 215 physics of nuclei and their low-lying excitations as dominated by only a few (typically one or
 216 two) collective shapes – equilibrium shapes with their vibrations – that rotate (Fig. 1).

217

By exploiting this almost perfect symmetry, the SA framework resolves the scale explo-
 218 sion problem in nuclear structure calculations, *i.e.*, the explosive growth in computational
 219 resource demands with increasing number of particles and model spaces size. We note that

220 the SA-NCSM uses the complete model space (that is, all possible shapes) as usually done in
 221 conventional shell models, but expands, in a prescribed way, only for those deformed con-
 222 figurations with vibrations that lie outside of the complete model space. This is critical for
 223 enhanced prolate deformation, since spherical and less deformed or oblate shapes easily de-
 224 velop in comparatively small model-space sizes.

225 The SA-NCSM, when combined with a high-precision realistic inter-nucleon interaction,
 226 provides *ab initio* predictions of nuclear observables. We often adopt the NNLO_{opt} chiral
 227 potential [50] that is used without 3N forces, which have been shown to contribute minimally
 228 to the 3- and 4-nucleon binding energy [50]. Chiral potentials are typically parameterized
 229 by two-nucleon (and three-nucleon) data, whereas the parameters, called the low-energy
 230 constants (LECs), remain unchanged and are not adjusted from one many-body system to
 231 another. This ensures a predictive power. At the next-to-next-to-leading order (NNLO), there
 232 are 14 LECs that enter into the chiral nucleon-nucleon (NN) potential. Our recent findings
 233 reveal the remarkable result that the chiral potential parameterizations have no significant
 234 effect on the dominant nuclear features, such as nuclear shape and the associated Sp(3, ℝ)
 235 symmetry, along with cluster formation (Fig. 2), but only slightly vary details in the nuclear
 236 wave functions, such as the contributions of the equilibrium deformation and its vibrations
 within the predominant nuclear shape (Fig. 2, left, inset) [51].

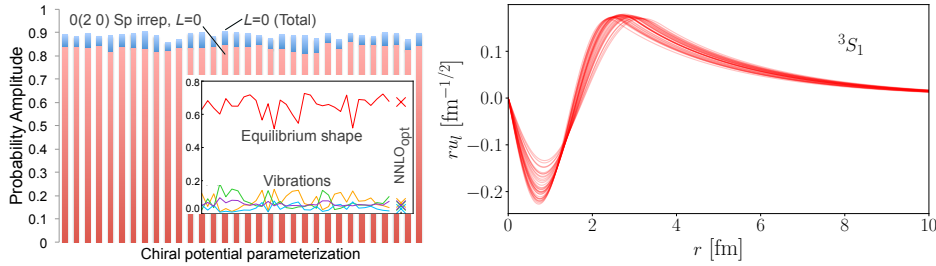


Figure 2: Chiral parameterization independence for nuclear shapes and cluster formation: (Left) Probability amplitude of the predominant Sp(3, ℝ) irrep $N_\sigma(\lambda_\sigma \mu_\sigma) = 0(2 0)$ ($L = 0$) in the ${}^6\text{Li } 1^+$ ground state. Inset: Contributions from the equilibrium shape (symplectic bandhead) and its vibrations (the case for the NNLO_{opt} is also shown). (Right) $\alpha + d$ 3S_1 -wave vs. the relative distance r . Calculated from the ${}^6\text{Li } 1^+$ ground state, computed with the SA-NCSM in the Sp(3, ℝ) scheme with NNLO chiral potential for 10 HO shells and $\hbar\Omega=15$ MeV. The $\pm 10\%$ variation in the LECs of the chiral potential is shown (left) on the horizontal axis and (right) by the spread of the curve. Figures adapted from [51].

237

238 3 Critical Role of Symmetries for Studies and Predictions of Nu- 239 clear Properties

240 3.1 Machine learning pattern recognition with the SA-NCSM

241 Machine learning approaches are ideal for pattern recognition, thereby providing a suitable
 242 framework to detect and utilize the highly organized patterns in atomic nuclei governed by
 243 the symplectic Sp(3, ℝ) symmetry.

244 Specifically, Ref. [31] introduces a novel machine learning approach to provide further
 245 insight into atomic nuclei and to detect orderly patterns amidst a vast data of large-scale
 246 calculations. The method utilizes a physics-informed neural network that is trained on *ab*

247 *initio* results from the SA-NCSM for light nuclei. Indeed, the SA-NCSM, which expands *ab*
 248 *initio* applications up to medium-mass nuclei, can reach even heavier nuclei when coupled
 249 with the machine learning approach. In particular, we find that a neural network trained on
 250 probability amplitudes for *s*- and *p*-shell nuclear wave functions not only predicts dominant
 251 configurations for heavier nuclei but in addition, when tested for the ^{20}Ne ground state, it
 accurately reproduces the probability distribution (Fig. 3).

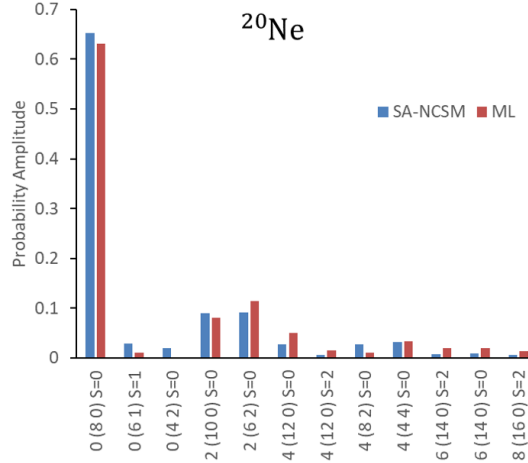


Figure 3: A novel machine learning approach coupled with the *ab initio* SA-NCSM is capable to detect orderly patterns amidst a vast data of large-scale calculations and to describe *sd*-shell nuclei, such as ^{20}Ne (shown), ^{24}Si , ^{40}Mg , and even the extremely heavy nuclei such as $^{166,168}\text{Er}$ and ^{236}U , by training only on nuclei up to ^{16}O . Figure from [31].

252

253

254

255

256

257

258

259

260

261

The nonnegligible configurations predicted by the network provide an important input to the SA-NCSM for reducing ultra-large model spaces to manageable sizes that can be, in turn, utilized in SA-NCSM calculations to obtain accurate observables. The neural network is capable of describing nuclear deformation and is used to track the shape evolution along the $^{20-42}\text{Mg}$ isotopic chain, suggesting a shape-coexistence that is more pronounced toward the very neutron-rich isotopes [31]. Furthermore, the neural network provides first descriptions of the structure and deformation of ^{24}Si and ^{40}Mg of interest to x-ray burst nucleosynthesis, and even of the extremely heavy nuclei such as $^{166,168}\text{Er}$ and ^{236}U , that build upon first principles considerations [31].

262

3.2 Probing clustering and physics beyond the standard model

263

264

265

266

267

268

269

270

271

272

The left-handed vector minus axial-vector (*V*–*A*) structure of the weak interaction was postulated in late 1950’s and early 1960’s guided in large part by a series of beta-decay experiments, and later was incorporated in the Standard Model of particle physics. However, in its most general form, the weak interaction can also have scalar, tensor, and pseudoscalar terms as well as right-handed currents. The β decay of ^8Li to ^8Be , which subsequently breaks up into two α particles, has long been recognized as an excellent testing ground to search for new physics (e.g. see [52]) due to the high decay energy and the ease of detecting the β and two α particles. These experiments have achieved remarkable precision (e.g., see [53,54]) that now requires confronting the systematic uncertainties that stem from the higher-order corrections in nuclear beta decay that are difficult to measure experimentally.

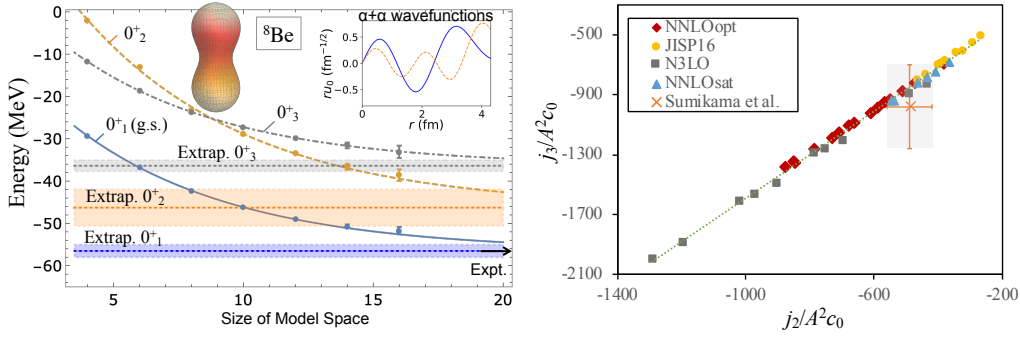


Figure 4: The *ab initio* SA-NCSM places unprecedented constraints on higher-(recoil-) order corrections (j_2/A^2c_0 and j_3/A^2c_0) in the β decay of ${}^8\text{Li}\rightarrow{}^8\text{Be}$ by addressing the challenging $\alpha + \alpha$ structure of ${}^8\text{Be}$. The results are essential for largely improving the sensitivity of high-precision experiments that probe the weak interaction theory and test physics beyond the Standard Model. Calculations performed on the NERSC and Frontera systems. Figures from [32] & [54].

273 As a remarkable result, the *ab initio* SA-NCSM has recently determined the size of the
 274 recoil-order form factors in the β decay of ${}^8\text{Li}$ (Fig. 4). It has shown that states of the $\alpha + \alpha$
 275 system not included in the evaluated ${}^8\text{Be}$ energy spectrum have an important effect on all
 276 $j_{2,3}/A^2c_0$, b/Ac_0 and d/Ac_0 recoil-order terms, and can explain the elusive M_{GT} discrepancy in
 277 the $A = 8$ systems common to all other *ab initio* approaches.

278 The SA-NCSM outcomes of Ref. [32] reduce – by over 50% – the uncertainty on these
 279 recoil-order corrections. These results help improve the sensitivity of high-precision β -decay
 280 experiments that probe the V–A structure of the weak interaction in the most stringent limit
 281 on tensor current contribution to the weak interaction theory to date, established in Ref. [54].
 282 Furthermore, the SA-NCSM predicted b/Ac_0 and d/Ac_0 values are important for other inves-
 283 tigations of the Standard Model symmetries, such as the conserved vector current hypothesis
 284 and the existence of second-class currents in the weak interaction.

285 3.3 Optical potential in the symmetry-adapted framework for nuclear reactions

286 In recent years there has been a significant interest in describing nuclear reactions from *ab*
 287 *initio* approaches, and especially in constructing from first principles effective inter-cluster
 288 interactions, often referred to as optical potentials. *Ab initio* optical potentials for elastic
 289 scattering at low energy are of particular interest for experiments at rare isotope beams. To
 290 utilize the efficacy of the symmetry-adapted basis, we combine the *ab initio* symmetry-adapted
 291 no-core shell model with the Green’s function technique (SANCSM/GF) and construct non-
 292 local optical potentials rooted in first principles [55,56]. Using the Green’s function technique
 293 ensures that all relevant cluster partitionings are included in the effective potential between
 294 the two reaction fragments (clusters) that are typically in their ground state in the entrance
 295 channel. With the view toward studying neutron and proton elastic scattering from deformed
 296 and heavy targets, we first examine a target of ${}^4\text{He}$ (Fig. 5a), where the effect of the spurious
 297 center-of-mass motion is most evident.

298 In a complementary symmetry-adapted resonating group method (SA-RGM) framework
 299 [58], one starts from an *ab initio* description of all particles involved and derives the effec-
 300 tive potential for localized clusters, which are properly normalized and orthogonalized in the
 301 particle sector, which yields non-local effective nucleon-nucleus interactions for the cluster
 302 partitioning or channel under consideration. For a single channel, if the effects of the target
 303 excitations are neglected, the non-local effective nucleon-nucleus interaction can be calcu-

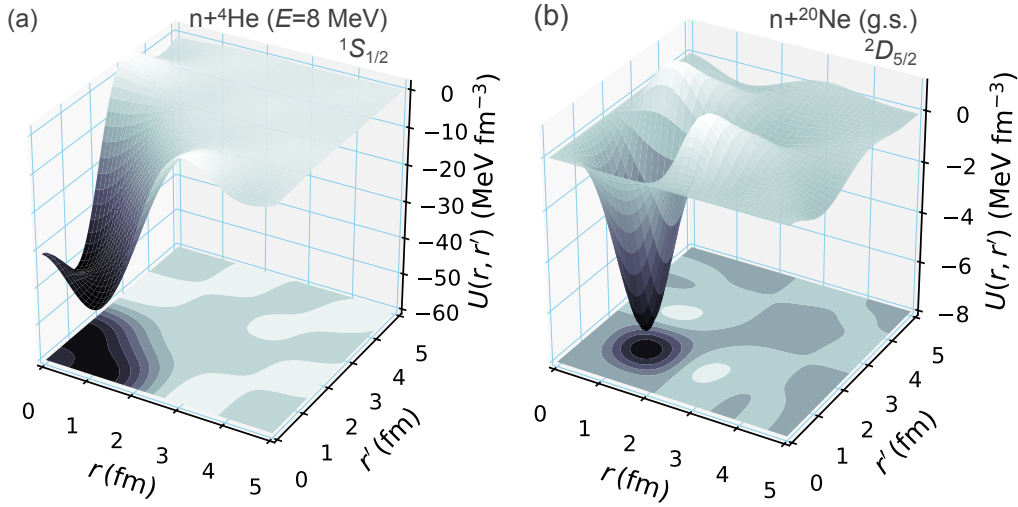


Figure 5: (a) Translationally invariant non-local optical potential for elastic neutron scattering for a ${}^4\text{He}$ target at $E = 8$ MeV center-of-mass energy, calculated in the SA-NCSM with the Green’s function technique (10 shells, $\hbar\Omega=17\text{MeV}$). Figure from [55]. (b) Effective neutron-nucleus non-local potential (translationally invariant) for the ${}^{20}\text{Ne}$ ground state, where effects of the target excitations and antisymmetrization involving three nucleons are neglected (based on *ab initio* SA-NCSM calculations of ${}^{20}\text{Ne}$ with NNLO_{opt} in a model space of 11 shells and $\hbar\Omega=15$ MeV inter-shell distance). Figure from [57].

304 lated for each partial wave, as illustrated for $n+{}^{20}\text{Ne}(0_{\text{g.s.}}^+)$ with NNLO_{opt} in 11 shells (Fig.
 305 5b). While these calculations limit the antisymmetrization to two nucleons only, this is a
 306 first step toward constructing effective nucleon-nucleus potentials for light and medium-mass
 307 nuclei for the astrophysically relevant energies [59, 60].

308 4 Conclusion

309 We have discussed the critical role of the emergent $\text{Sp}(3, \mathbb{R})$ symmetry in atomic nuclei and
 310 the associated subgroup $\text{SU}(3)$, which in turn underpin the $\text{Sp}(3, \mathbb{R})$ and $\text{SU}(3)$ schemes.
 311 By exploiting these schemes, the *ab initio* SA-NCSM has enabled machine-learning pattern
 312 recognition and descriptions of heavy nuclei, *ab initio* modeling of α clustering and collectivity,
 313 along with tests of beyond-the-standard-model physics. In addition, we show that with the
 314 help of the SA-NCSM, which expands *ab initio* applications up to medium-mass nuclei by using
 315 the dominant symmetry of nuclear dynamics, one can provide solutions to reaction processes
 316 in this region, with a focus on elastic neutron scattering.

317 Acknowledgements

318 We are grateful to J. E. Escher, A. Ekström, D. Rowe, G. Rosensteel, and J. Wood for useful
 319 discussions, as well as to N.D. Scielzo, M.T. Burkey, A.T. Gallant, G. Savard, and collaborators
 320 for motivating and providing important insights on the ${}^8\text{Li}$ decay study.

321 **Funding information** This work was supported in part by the U.S. National Science Founda-
322 tion (PHY-1913728, PHY-2209060), the U.S. Department of Energy (DE-SC0019521) and the
323 Czech Science Foundation (22-14497S). This work was performed under the auspices of the
324 U.S. Department of Energy by Lawrence Livermore National Laboratory under Contract DE-
325 AC52-07NA27344 and the National Nuclear Security Administration through the Center for
326 Excellence in Nuclear Training and University Based Research (CENTAUR) under Grant No.
327 DE-NA0003841. This work benefited from high performance computational resources pro-
328 vided by LSU (www.hpc.lsu.edu), the National Energy Research Scientific Computing Center
329 (NERSC), a U.S. Department of Energy Office of Science User Facility operated under Contract
330 No. DE-AC02-05CH11231, as well as the Frontera computing project at the Texas Advanced
331 Computing Center, made possible by National Science Foundation award OAC-1818253.

332 References

- 333 [1] T. Dytrych, K. D. Launey, J. P. Draayer, D. J. Rowe, J. L. Wood, G. Rosensteel, C. Bahri,
334 D. Langr and R. B. Baker, *Physics of nuclei: Key role of an emergent symmetry*, Phys. Rev.
335 Lett. **124**, 042501 (2020), doi:[10.1103/PhysRevLett.124.042501](https://doi.org/10.1103/PhysRevLett.124.042501).
- 336 [2] G. Rosensteel and D. J. Rowe, *Nuclear Sp(3,R) Model*, Phys. Rev. Lett. **38**, 10 (1977).
- 337 [3] J. Draayer, K. Weeks and G. Rosensteel, *Symplectic Shell-model Calculations for ^{20}Ne with*
338 *Horizontal Configuration Mixing*, Nucl. Phys. **A413**, 215 (1984).
- 339 [4] D. J. Rowe, *Microscopic theory of the nuclear collective model*, Reports on Progr. in Phys.
340 **48**, 1419 (1985).
- 341 [5] J. P. Draayer and Y. Akiyama, *Wigner and Racah Coefficients for SU(3)*, J. Math. Phys.
342 **14**, 1904 (1973).
- 343 [6] A. Blokhin, C. Bahri and J. Draayer, Phys. Rev. Lett. **74**, 4149 (1995).
- 344 [7] K. D. Launey, T. Dytrych and J. P. Draayer, *Symmetry-guided large-scale shell-model theory*,
345 Prog. Part. Nucl. Phys. **89**, 101 (review) (2016), doi:[10.1016/j.pnpnp.2016.02.001](https://doi.org/10.1016/j.pnpnp.2016.02.001).
- 346 [8] G. Rosensteel and D. J. Rowe, Ann. Phys. N.Y. **126**, 343 (1980).
- 347 [9] D. J. Rowe, *Dynamical symmetries of nuclear collective models*, Prog. Part. Nucl. Phys.
348 **37**, 265 (1996).
- 349 [10] K. Heyde and J. L. Wood, *Shape coexistence in atomic nuclei*, Rev. Mod. Phys. **83**, 1467
350 (2011).
- 351 [11] J. L. Wood, *Nuclear Collectivity – its emergent nature viewed from phenomenology and*
352 *spectroscopy*, In *Emergent phenomena in atomic nuclei from large-scale modeling: a*
353 *symmetry-guided perspective*, p. 3. World Scientific Publishing Co., ISBN 978-981-3146-
354 04-4, 978-981-3146-06-8, doi:[10.1142/9789813146051_0001](https://doi.org/10.1142/9789813146051_0001) (2017).
- 355 [12] D. J. Rowe and J. L. Wood, *A relationship between isobaric analog states and shape*
356 *coexistence in nuclei*, J. Phys. G: Nucl. Part. Phys. **45**(6), 06LT01 (2018).
- 357 [13] J. P. Elliott, *Collective Motion in the Nuclear Shell Model. I. Classification Schemes for*
358 *States of Mixed Configurations*, Proc. Roy. Soc. A **245**, 128 (1958).

- 359 [14] J. P. Elliott, *Collective Motion in the Nuclear Shell Model. II. The Introduction of Intrinsic*
360 *Wave-Functions*, Proc. Roy. Soc. A **245**, 562 (1958).
- 361 [15] J. P. Elliott and M. Harvey, *Collective Motion in the Nuclear Shell Model. III. The Calculation*
362 *of Spectra*, Proc. Roy. Soc. A **272**, 557 (1963).
- 363 [16] K. T. Hecht and A. Adler, Nucl. Phys. A **A137**, 129 (1969).
- 364 [17] K. T. Hecht and W. Zahn, *An $SU(3)$ approach to nuclear multi-cluster problems*, Nucl.
365 Phys. A **318**, 1 (1979).
- 366 [18] C. Bahri and D. J. Rowe, *$Su(3)$ quasi-dynamical symmetry as an organizational mecha-*
367 *nism for generating nuclear rotational motions*, Nucl. Phys. A **662**, 125 (2000).
- 368 [19] T. Dytrych, K. D. Sviratcheva, C. Bahri, J. P. Draayer and J. P. Vary, *Evidence for Symplectic*
369 *Symmetry in ab initio No-core-shell-model Results for Light Nuclei*, Phys. Rev. Lett. **98**,
370 162503 (2007).
- 371 [20] T. Dytrych, K. D. Launey, J. P. Draayer, P. Maris, J. P. Vary, E. Saule, U. Catalyurek,
372 M. Sosonkina, D. Langr and M. A. Caprio, *Collective Modes in Light Nuclei from First*
373 *Principles*, Phys. Rev. Lett. **111**, 252501 (2013), doi:[10.1103/PhysRevLett.111.252501](https://doi.org/10.1103/PhysRevLett.111.252501).
- 374 [21] P. F. Bedaque and U. van Kolck, *Effective field theory for few-nucleon systems*, Annu. Rev.
375 Nucl. Part. Sci. **52**(1), 339 (2002), doi:[10.1146/annurev.nucl.52.050102.090637](https://doi.org/10.1146/annurev.nucl.52.050102.090637).
- 376 [22] E. Epelbaum, A. Nogga, W. Glöckle, H. Kamada, U.-G. Meißner and H. Witala, *Three-*
377 *nucleon forces from chiral effective field theory*, Phys. Rev. C **66**, 064001 (2002).
- 378 [23] D. R. Entem and R. Machleidt, Phys. Rev. C **68**, 041001 (2003).
- 379 [24] T. Dytrych, P. Maris, K. D. Launey, J. P. Draayer, J. P. Vary, M. Caprio, D. Langr,
380 U. Catalyurek and M. Sosonkina, *Efficacy of the $SU(3)$ scheme for ab initio large-scale*
381 *calculations beyond the lightest nuclei*, Comput. Phys. Commun. **207**, 202 (2016),
382 doi:[10.1016/j.cpc.2016.06.006](https://doi.org/10.1016/j.cpc.2016.06.006).
- 383 [25] T. Dytrych, A. C. Hayes, K. D. Launey, J. P. Draayer, P. Maris, J. P. Vary, D. Langr and
384 T. Oberhuber, *Electron-scattering form factors for ${}^6\text{Li}$ in the ab initio symmetry-guided*
385 *framework*, Phys. Rev. C **91**, 024326 (2015), doi:[10.1103/PhysRevC.91.024326](https://doi.org/10.1103/PhysRevC.91.024326).
- 386 [26] R. B. Baker, K. D. Launey, S. Bacca, N. N. Dinur and T. Dytrych, *Benchmark calculations*
387 *of electromagnetic sum rules with a symmetry-adapted basis and hyperspherical harmonics*,
388 Phys. Rev. C **102**, 014320 (2020), doi:[10.1103/PhysRevC.102.014320](https://doi.org/10.1103/PhysRevC.102.014320).
- 389 [27] P. Ruotsalainen, J. Henderson, G. Hackman, G. H. Sargsyan, K. D. Launey, A. Saxena,
390 P. C. Srivastava, S. R. Stroberg, T. Grahm, J. Pakarinen, G. C. Ball, R. Julin *et al.*, *Isospin*
391 *symmetry in $b(e2)$ values: Coulomb excitation study of ${}^{21}\text{Mg}$* , Phys. Rev. C **99**, 051301
392 (2019), doi:[10.1103/PhysRevC.99.051301](https://doi.org/10.1103/PhysRevC.99.051301).
- 393 [28] J. Henderson *et al.*, *Testing microscopically derived descriptions of nuclear*
394 *collectivity: Coulomb excitation of ${}^{22}\text{Mg}$* , Phys. Lett. **B782**, 468 (2018),
395 doi:[10.1016/j.physletb.2018.05.064](https://doi.org/10.1016/j.physletb.2018.05.064), [1709.03948](https://arxiv.org/abs/1709.03948).
- 396 [29] J. Williams, G. C. Ball, A. Chester, T. Domingo, A. B. Garnsworthy, G. Hackman, J. Hen-
397 derson, R. Henderson, R. Krücken, A. Kumar, K. D. Launey, J. Measures *et al.*, *Struc-*
398 *ture of ${}^{28}\text{Mg}$ and influence of the neutron pf shell*, Phys. Rev. C **100**, 014322 (2019),
399 doi:[10.1103/PhysRevC.100.014322](https://doi.org/10.1103/PhysRevC.100.014322).

- 400 [30] K. D. Launey, A. Mercenne, G. H. Sargsyan, H. Shows, R. B. Baker, M. E. Miora,
401 T. Dytrych and J. P. Draayer, *Emergent clustering phenomena in the framework of the*
402 *ab initio symmetry-adapted no-core shell model*, In *Proceedings of the 4th International*
403 *Workshop on 'State of the Art in Nuclear Cluster Physics' (SOTANCP4), May 2018, Galve-*
404 *ston, Texas*, vol. 2038. AIP Conference Proceedings (2018).
- 405 [31] O. M. Molchanov, K. D. Launey, A. Mercenne, G. H. Sargsyan, T. Dytrych and J. P.
406 Draayer, *Machine learning approach to pattern recognition in nuclear dynamics from*
407 *the ab initio symmetry-adapted no-core shell model*, *Phys. Rev. C* **105**, 034306 (2022),
408 doi:[10.1103/PhysRevC.105.034306](https://doi.org/10.1103/PhysRevC.105.034306).
- 409 [32] G. H. Sargsyan, K. D. Launey, M. T. Burkey, A. T. Gallant, N. D. Scielzo, G. Savard,
410 A. Mercenne, T. Dytrych, D. Langr, L. Varriano, B. Longfellow, T. Y. Hirsh *et al.*, *Impact of*
411 *clustering on the ^8Li β decay and recoil form factors*, *Phys. Rev. Lett.* **128**, 202503 (2022),
412 doi:[10.1103/PhysRevLett.128.202503](https://doi.org/10.1103/PhysRevLett.128.202503).
- 413 [33] M. Moshinsky, *Wigner Coefficients for the SU_3 Group and Some Applications*, *Rev. Mod.*
414 *Phys.* **34**, 813 (1962).
- 415 [34] M. Moshinsky, J. Patera, R. T. Sharp and P. Winternitz, *Everything you always wanted to*
416 *know about $SU(3) \supset O(3)$* , *Ann. Phys. (N.Y.)* **95**, 139 (1975).
- 417 [35] V. K. B. Kota, *$SU(3)$ Symmetry in Atomic Nuclei*, Springer Singapore, ISBN 978-981-15-
418 3602-1, doi:[10.1007/978-981-15-3603-8](https://doi.org/10.1007/978-981-15-3603-8) (2020).
- 419 [36] G. Rosensteel and D. J. Rowe, *Ann. Phys. N.Y.* **104**, 134 (1977).
- 420 [37] Y. Leschber and J. P. Draayer, *Phys. Letts. B* **190**, 1 (1987).
- 421 [38] O. Castaños, J. P. Draayer and Y. Leschber, *Z. Phys. A* **329**, 33 (1988).
- 422 [39] D. J. Rowe and J. L. Wood, *Fundamentals of nuclear models: foundational models*, World
423 Scientific, Singapore (2010).
- 424 [40] J. P. Draayer, Y. Leschber, S. C. Park and R. Lopez, *Representations of $U(3)$ in $U(N)$* ,
425 *Comput. Phys. Commun.* **56**, 279 (1989).
- 426 [41] D. Rowe, *The fundamental role of symmetry in nuclear models*, *AIP Conf. Proc.* **1541**,
427 104 (2013).
- 428 [42] T. Dytrych, K. D. Sviratcheva, J. P. Draayer, C. Bahri and J. P. Vary, *Ab initio symplectic*
429 *no-core shell model*, *J. Phys. G: Nucl. Part. Phys.* **35**, 123101 (2008).
- 430 [43] J. Escher and J. P. Draayer, *J. Math. Phys.* **39**, 5123 (1998).
- 431 [44] D. J. Rowe, G. Thiamova and J. L. Wood, *Implications of Deformation and Shape Coexis-*
432 *tence for the Nuclear Shell Model*, *Phys. Rev. Lett.* **97**, 202501 (2006).
- 433 [45] A. C. Dreyfuss, K. D. Launey, T. Dytrych, J. P. Draayer and C. Bahri, *Hoyle state and*
434 *rotational features in Carbon-12 within a no-core shell model framework*, *Phys. Lett. B*
435 **727**, 511 (2013).
- 436 [46] G. K. Tobin, M. C. Ferriss, K. D. Launey, T. Dytrych, J. P. Draayer and C. Bahri, *Symplec-*
437 *tic No-core Shell-model Approach to Intermediate-mass Nuclei*, *Phys. Rev. C* **89**, 034312
438 (2014).
- 439 [47] O. Castaños, P. Hess, J. Draayer and P. Rochford, *Nucl. Phys. A* **524**, 469 (1991).

- 440 [48] M. Jarrío, J. L. Wood and D. J. Rowe, *The SU(3) structure of rotational states in heavy*
441 *deformed nuclei*, Nucl. Phys. A **528**, 409 (1991).
- 442 [49] M. Freer, H. Horiuchi, Y. Kanada-En'yo, D. Lee and U.-G. Meißner, *Microscopic*
443 *clustering in light nuclei*, Rev. Mod. Phys. **90**, 035004 (2018),
444 doi:[10.1103/RevModPhys.90.035004](https://doi.org/10.1103/RevModPhys.90.035004).
- 445 [50] A. Ekström, G. Baardsen, C. Forssén, G. Hagen, M. Hjorth-Jensen, G. R. Jansen, R. Mach-
446 leidt, W. Nazarewicz *et al.*, *An optimized chiral nucleon-nucleon interaction at next-to-*
447 *next-to-leading order*, Phys. Rev. Lett. **110**, 192502 (2013).
- 448 [51] K. S. Becker, K. D. Launey, A. Ekstrom and T. Dytrych, *Ab initio symmetry-adapted*
449 *emulator for studying emergent collectivity and clustering in nuclei*, Frontiers (submitted)
450 (2022).
- 451 [52] B. R. Holstein, *Recoil effects in allowed beta decay: The elementary particle approach*, Rev.
452 Mod. Phys. **46**, 789 (1974), doi:[10.1103/RevModPhys.46.789](https://doi.org/10.1103/RevModPhys.46.789).
- 453 [53] M. Sternberg, R. Segel, N. Scielzo, G. Savard, J. Clark, P. Bertone, F. Buchinger,
454 M. Burkey, S. Caldwell, A. Chaudhuri *et al.*, *Limit on tensor currents from ^8Li β de-*
455 *cay*, Phys. Rev. Lett. **115**(18), 182501 (2015).
- 456 [54] M. T. Burkey, G. Savard, A. T. Gallant, N. D. Scielzo, J. A. Clark, T. Y. Hirsh, L. Varriano,
457 G. H. Sargsyan, K. D. Launey, M. Brodeur, D. P. Burdette, E. Heckmaier *et al.*, *Improved*
458 *limit on tensor currents in the weak interaction from ^8Li β decay*, Phys. Rev. Lett. **128**,
459 202502 (2022), doi:[10.1103/PhysRevLett.128.202502](https://doi.org/10.1103/PhysRevLett.128.202502).
- 460 [55] M. B. Burrows, K. D. Launey *et al.*, *Ab initio low-energy optical potentials from the*
461 *symmetry-adapted no-core shell model*, (in preparation) (2022).
- 462 [56] M. B. Burrows, K. D. Launey *et al.*, *Ab initio optical potentials for elastic scattering at low*
463 *energies using the symmetry-adapted no-core shell model*, 2021 Fall Meeting of the Divi-
464 sion of Nuclear Physics, APS (meetings.aps.org/Meeting/DNP21/Session/KM.3)
465 (2021).
- 466 [57] K. D. Launey, A. Mercenne and T. Dytrych, *Nuclear dynamics and reactions in the*
467 *ab initio symmetry-adapted framework*, Annu. Rev. Nucl. Part. Sci. **71**, 253 (2021),
468 doi:[10.1146/annurev-nucl-102419-033316](https://doi.org/10.1146/annurev-nucl-102419-033316).
- 469 [58] A. Mercenne, K. Launey, T. Dytrych, J. Escher, S. Quaglioni, G. Sargsyan, D. Langr and
470 J. Draayer, *Efficacy of the symmetry-adapted basis for ab initio nucleon-nucleus interactions*
471 *for light- and intermediate-mass nuclei*, Computer Physics Communications **280**, 108476
472 (2022), doi:<https://doi.org/10.1016/j.cpc.2022.108476>.
- 473 [59] A. Mercenne, K. D. Launey, J. E. Escher, T. Dytrych and J. P. Draayer, *New Ab Initio*
474 *Approach to Nuclear Reactions Based on the Symmetry-Adapted No-Core Shell Model*, In
475 N. Orr, M. Ploszajczak, F. Marques and J. Carbonell, eds., *Recent Progress in Few-Body*
476 *Physics*, vol. 238, p. 253. Springer Proc. Phys., doi:[https://doi.org/10.1007/978-3-030-](https://doi.org/10.1007/978-3-030-32357-8_44)
477 [32357-8_44](https://doi.org/10.1007/978-3-030-32357-8_44) (2020).
- 478 [60] A. Mercenne, K. D. Launey, J. E. Escher, T. Dytrych and J. P. Draayer, *New ab initio ap-*
479 *proach to nuclear reactions based on the symmetry-adapted no-core shell model*, In J. Es-
480 cher, ed., *Proceedings of the 6th International Workshop on Compound-Nuclear Reactions*
481 *and Related Topics (CNR*18)*, p. 73. Berlin: Springer (2021).